nature nanotechnology

SUPPLEMENTARY INFORMATION

https://doi.org/10.1038/s41565-020-0648-y

In the format provided by the authors and unedited.

Dual-targeting nanoparticle vaccine elicits a therapeutic antibody response against chronic hepatitis B

Wenjun Wang[1,2], Xiaoxiao Zhou[1,2], Yingjie Bian[1], Shan Wang[3], Qian Chai[1], Zhenqian Guo[3], Zhenni Wang[3], Ping Zhu[4], Hua Peng[1], Xiyun Yan[5], Wenhui Li[6], Yang-Xin Fu[7] and Mingzhao Zhu[1,2] ✉

[1]Key Laboratory of Infection and Immunity, Institute of Biophysics, Chinese Academy of Sciences, Beijing, China. [2]College of Life Sciences, University of the Chinese Academy of Sciences, Beijing, China. [3]Department of Pediatric Surgical Oncology, Children's Hospital, Chongqing Medical University, Chongqing, China. [4]National Laboratory of Biomacromolecules, Institute of Biophysics, Chinese Academy of Sciences, Beijing, China. [5]Key Laboratory of Protein and Peptide Pharmaceutical, Institute of Biophysics, Chinese Academy of Sciences, Beijing, China. [6]National Institute of Biological Sciences, Beijing, China. [7]Department of Pathology, University of Texas Southwestern Medical Center, Dallas, TX, USA. ✉e-mail: zhumz@ibp.ac.cn

Dual-targeting nanoparticle vaccine elicits a therapeutic antibody response against chronic hepatitis B

Wenjun Wang[1, 2], Xiaoxiao Zhou[1, 2], Yingjie Bian[1], Shan Wang[3], Qian Chai[1], Zhenqian Guo[3], Zhenni Wang[3], Ping Zhu[4], Hua Peng[1], Xiyun Yan[5], Wenhui Li[6], Yang-Xin Fu[7] & Mingzhao Zhu[1, 2 *]

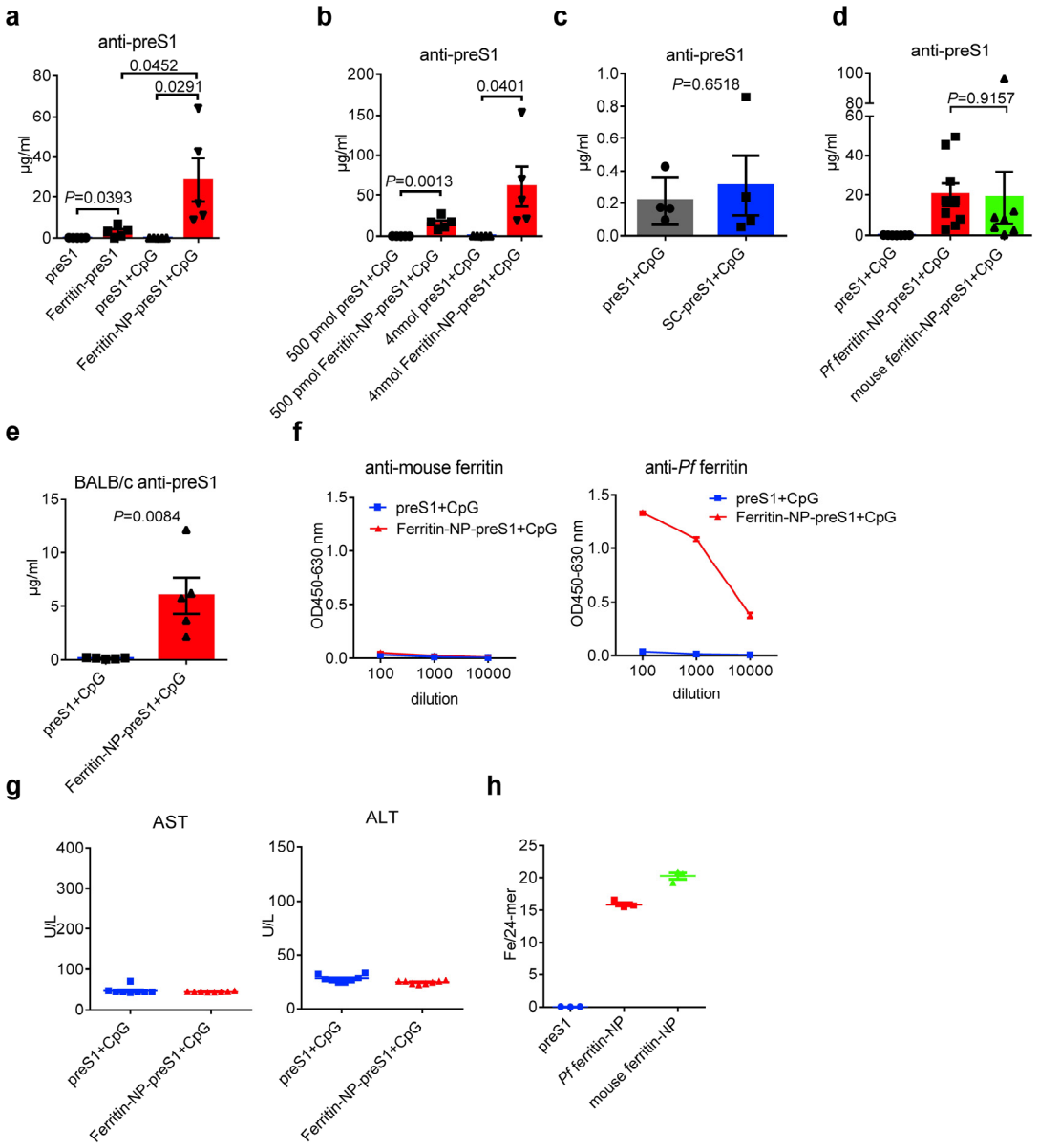

Supplementary Fig. 1: Ferritin-NP-preS1 vaccine is efficient and bio-safe. **a,** Naïve WT C57BL/6 mice (n=5) were subcutaneously immunized with 500 pmol ferritin-NP-preS1 or equimolar SC-preS1 subcutaneously with or without 30 μg CpG-1826 adjuvant at day 0 and 14. Anti-preS1 response was detected at day 21. **b,** Naïve WT C57BL/6 mice (n=5) were subcutaneously immunized with 500 pmol or 4 nmol ferritin-NP-preS1 or equimolar SC-preS1 soluble antigen with 30 μg CpG-1826 adjuvant at day 0 and 14. Anti-preS1 response was detected at day21. **c,** 500 pmol SC-preS1 or preS1 were subcutaneously immunized with 30 μg CpG-1826 adjuvant at day 0 and 14 (n=4). Anti-preS1 response was detected at day21. **d,** Anti-preS1 response at day 21 upon immunization with 500 pmol SC-preS1 (n=7), equimolar *Pf* ferritin-NP-preS1 (n=9) or mouse ferritin-NP-preS1 vaccine (n=7) were detected. **e,** Naïve WT BALB/c mice (n=5) were subcutaneously immunized with 500 pmol ferritin-NP-preS1 or equimolar SC-preS1 soluble antigen with 30 μg CpG-1826 adjuvant at day 0 and 14. Anti-preS1 response was detected at day 21. **f,** Antibody response against *Pf* ferritin and

mouse ferritin in SC-preS1 (n=6) or *Pf* ferritin NP vaccine (n=10) immunized mice at day 21. **g,** ALT and AST in sera collected at day 21 from vaccine immunized mice were measured (n=8). **h,** The iron content in ferritin NP (n=3). **a-f** are representative results of three independent experiments. **g** and **h** are representative results of two independent experiments. Data are shown as mean ± SEM. In **a-e**, statistical significance was determined by unpaired two-tailed *t*-test.

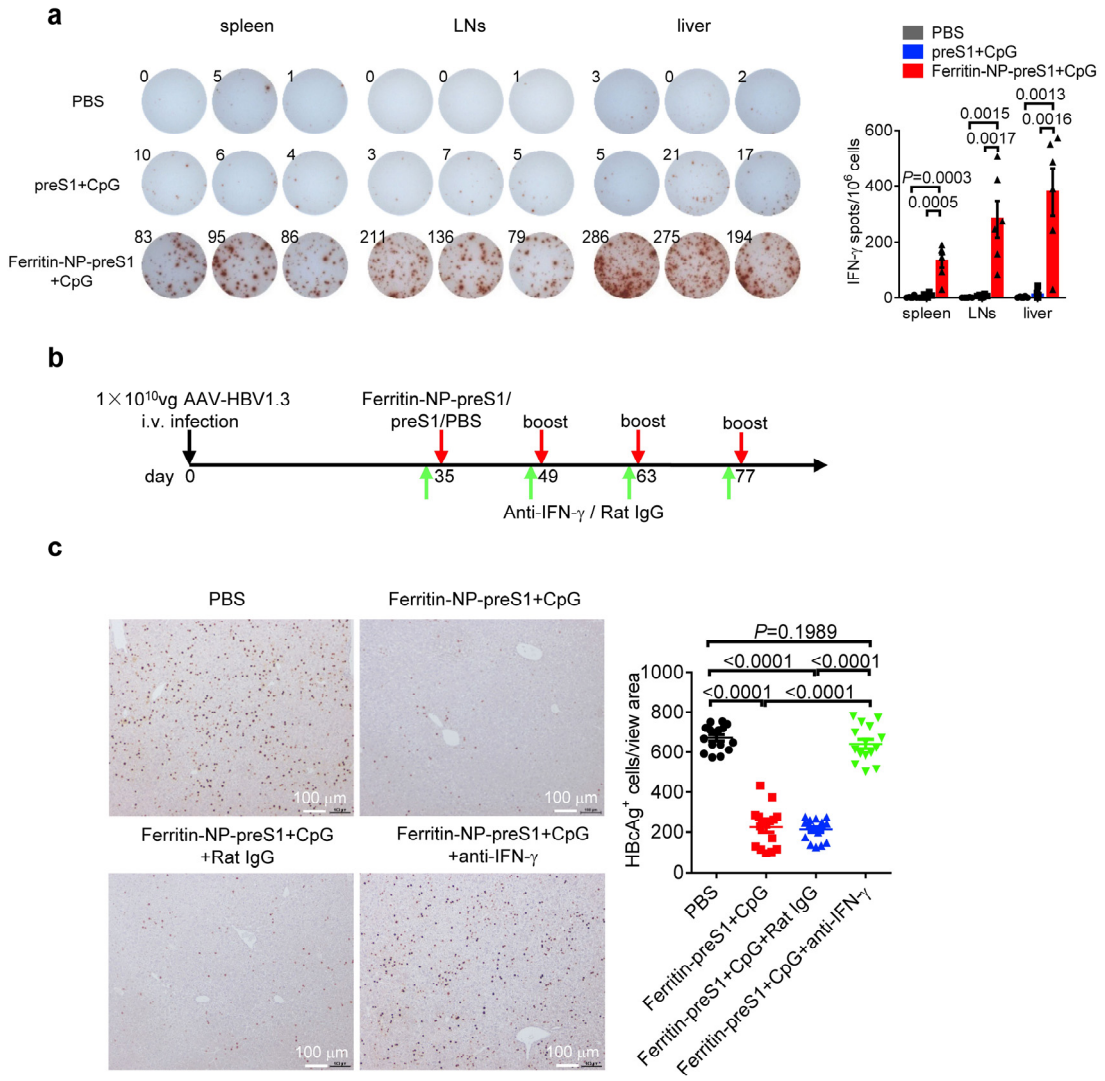

Supplementary Fig. 2: The therapeutic effect of ferritin-NP-preS1 vaccine depends on IFN-γ.

a, Stable HBV carrier mice (n=6) were vaccinated with ferritin-NP-preS1 vaccine or equimolar SC-preS1 soluble antigen regularly as in Fig. 3. Mice were sacrificed on the last day (day147), and 5×10^5 lymphocytes from LNs, spleen and liver were collected. Then, cells were stimulated with preS1 polypeptide for 48h. PreS1 specific IFNγ secretion was measured by ELISPOT assay. Data are representative results of two independent experiments. **b**, C57BL/6 mice (n=6) were inoculated with 1×10^{10} vg AAV-HBV1.3 virus intravenously. After 5 weeks, stable HBV carrier mice were vaccinated with 500 pmol ferritin-NP-preS1 vaccine with 30 μg CpG-1826 adjuvant for 4 times every 2 weeks as in Fig. 3. The IFN-γ blocking antibody (XMG1.2) or Rat IgG was administrated i.p. for 4 times the day before each vaccination. **c**, Immunological histological chemistry (IHC) staining for HBcAg in hepatocytes at day 147. Positive cells were counted by ImageJ software (n=16 section fields). Scale bar, 100 μm. Data are representative results of three independent experiments. In **a** and **c**, data are shown as mean ± SEM, statistical significance was determined by unpaired two-tailed *t*-test.

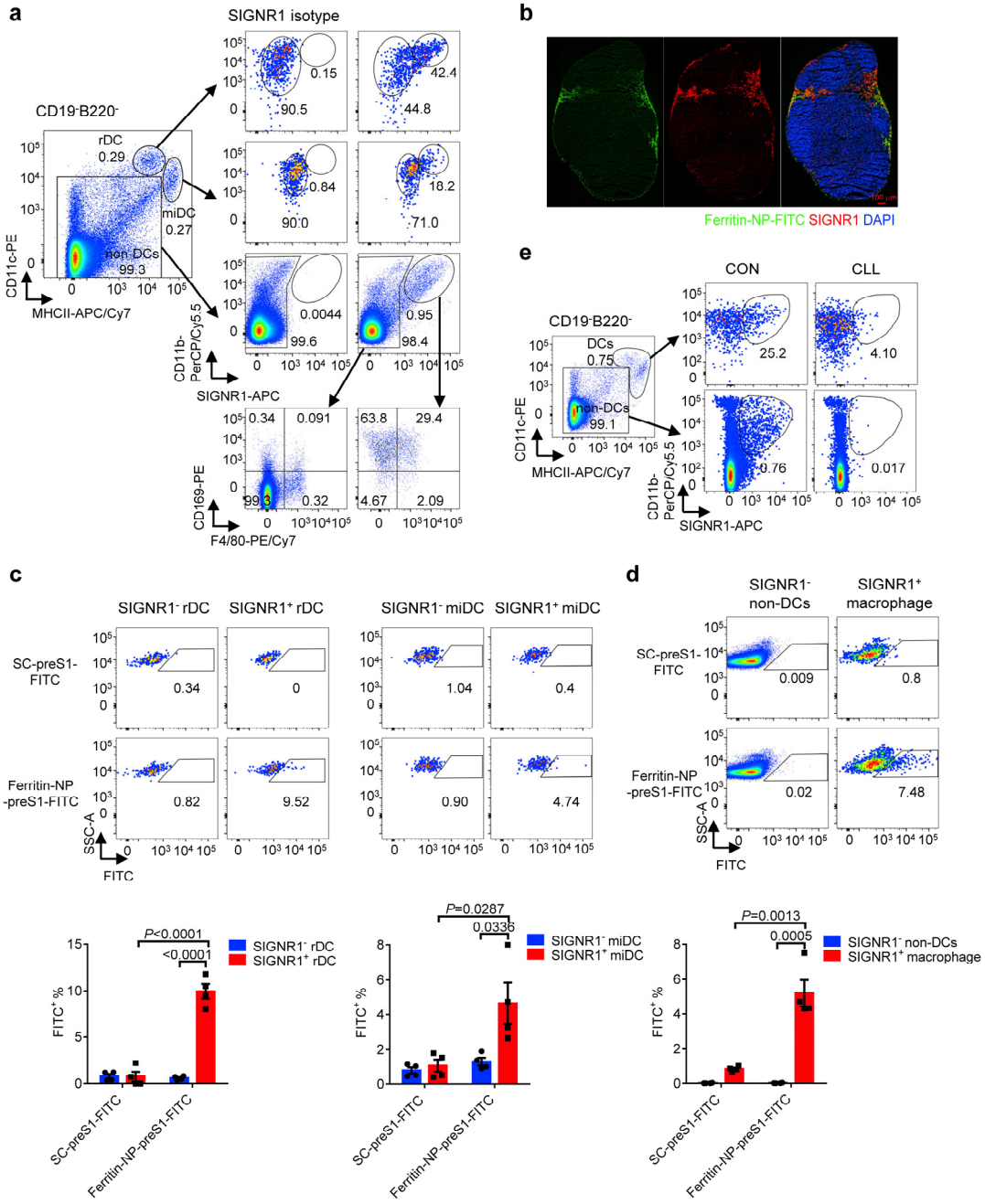

Supplementary Fig. 3: Ferritin-NP targets SIGNR1$^+$ APCs.

a, Inguinal LNs were digested into single cells, CD19$^-$B220$^-$ non-B cells were identified into three distinct populations: resident DC (rDC, CD11c^{hi}MHCII$^+$), migratory DC (miDC, CD11c$^+$MHCII^{hi}) and non-DC. Surface expression of SIGNR1 and CD11b by these three populations were analyzed. Among the non-DC population, SIGNR1$^+$ and SIGNR1$^-$ cells were analyzed by anti-F4/80 and anti-CD169 further. Numbers adjacent to the outlined areas indicate percent of each gate. The data show representative results of at least three independent experiments. **b,** C57BL/6 mice were subcutaneously injected with 2 nmol ferritin-NP-preS1-FITC. 4h after injection, cryo-sections of inguinal LNs were obtained. The section was stained with anti-SIGNR1 (red) and DAPI (blue). The data are representative results of three independent experiments. **c,d,**

C57BL/6 mice (n=4) were subcutaneously injected with 2 nmol ferritin-NP-preS1-FITC or equimolar SC-preS1-FITC. 4h after injection, ferritin-NP-preS1-FITC or SC-preS1-FITC capture of indicated DCs (**c**) or non-DCs (**d**) in iLN were presented and statistically analyzed. **c** and **d** are representative results of two independent experiments. Data are shown as mean ± SEM, statistical significance was determined by unpaired two-tailed *t*-test. **e,** 10 days post clodronate liposome (CLL) or control liposome (CON) f.p. injection, depletion of SIGNR1^{+} cells in pLN was determined by flow cytometry. The data are representative results of three independent experiments.

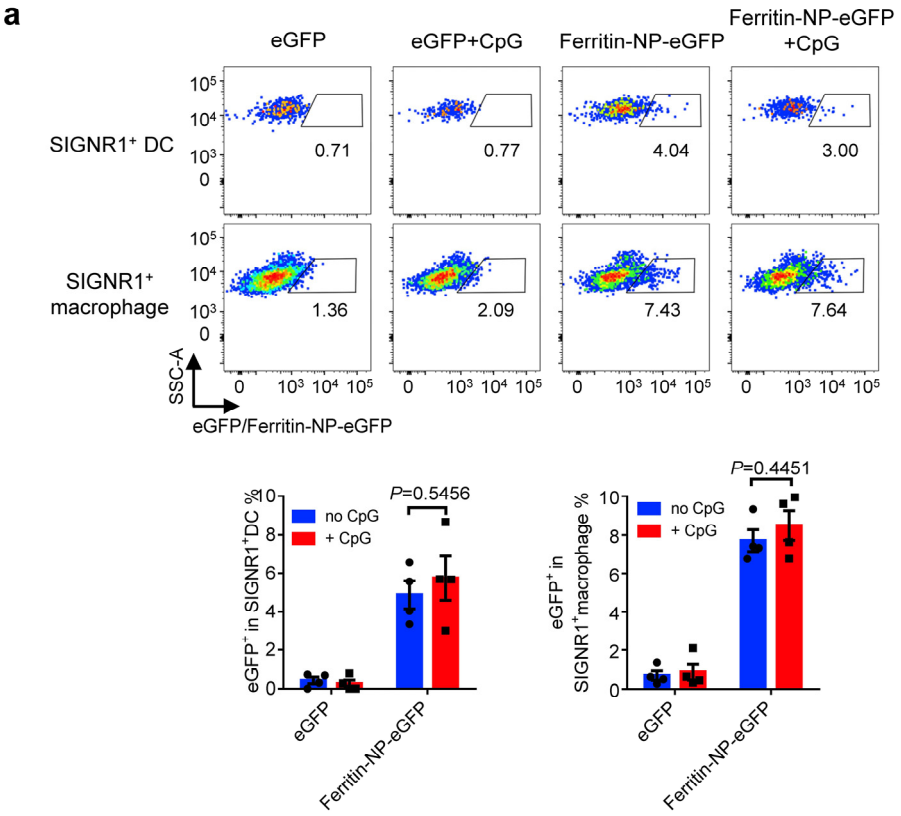

Supplementary Fig. 4: CpG-1826 adjuvant has no effect on ferritin-NP capture. **a,** C57BL/6 mice (n=4) were subcutaneously injected with 2 nmol ferritin-NP-eGFP or equimolar eGFP-SpyTag with or without 30μg CpG-1826 adjuvant. 4h after injection, inguinal LNs were digested into single cells, ferritin-NP-eGFP or eGFP-SpyTag capture by SIGNR1$^+$ DCs and SIGNR1$^+$ macrophages were presented and statistically analyzed. Data are representative results of two independent experiments. Data are shown as mean ± SEM, statistical significance was determined by unpaired two-tailed *t*-test.

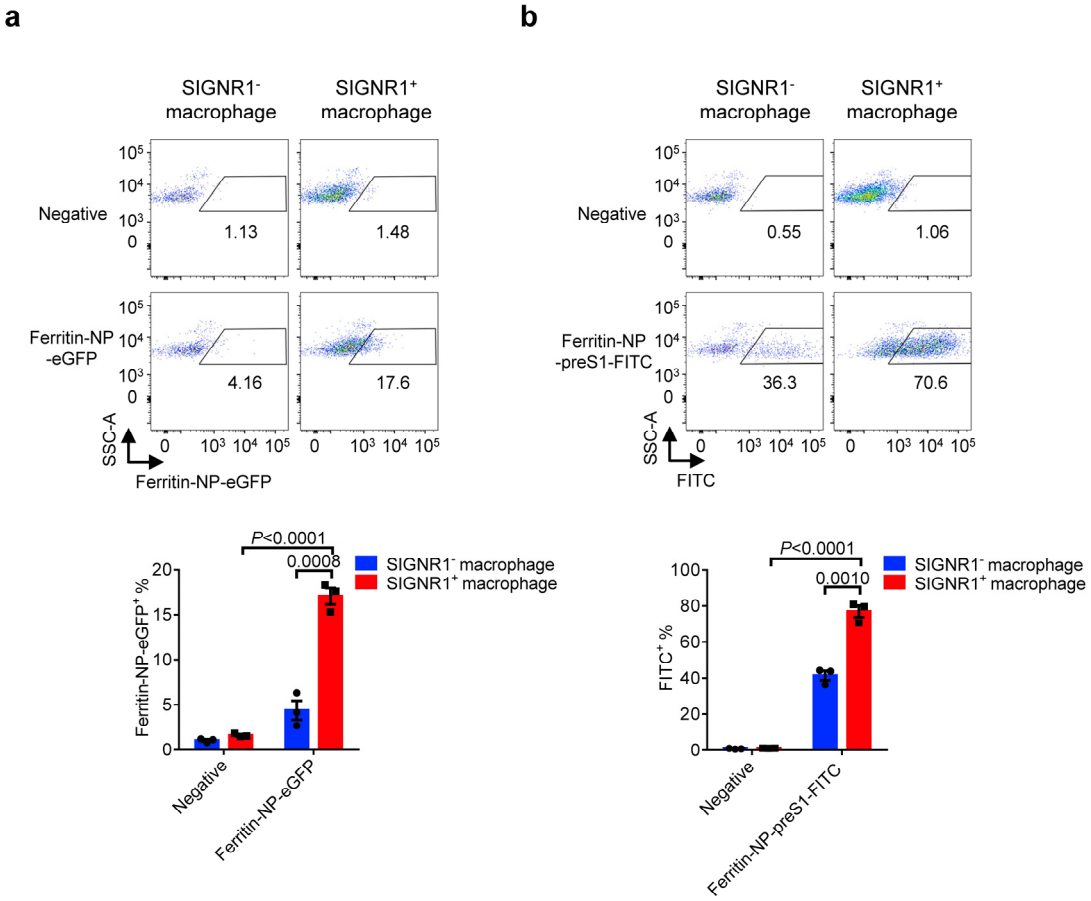

Supplementary Fig. 5: Ferritin-NP targets SIGNR1⁺ APCs *in vitro*.
a,b, Inguinal LNs from C57BL/6 WT mice were digested into single cells and incubated with ferritin-NP-eGFP (**a**) or ferritin-NP-preS1-FITC (**b**) *in vitro* (n=3). Ferritin-NP capture by $CD11c^{-}CD11b^{+}SIGNR1^{-}$ macrophages or $CD11c^{-}CD11b^{+}SIGNR1^{+}$ macrophages were presented and statistically analyzed. Data are representative results of three independent experiments. Data are shown as mean ± SEM, statistical significance was determined by unpaired two-tailed *t*-test.

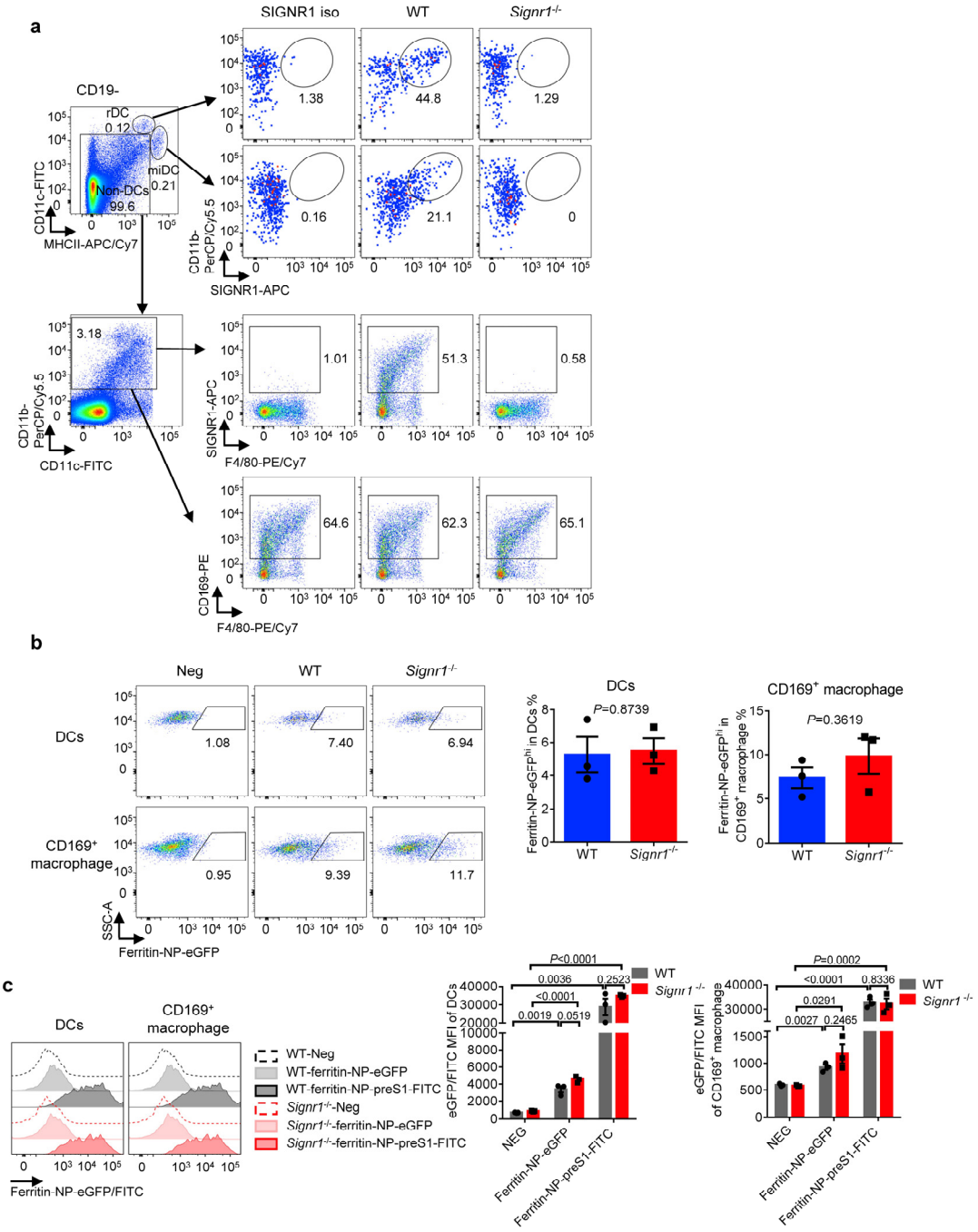

Supplementary Fig. 6: Ferritin-NP targeting in *Signr1*$^{-/-}$ mice.

a, Inguinal LNs from WT or *Signr1*$^{-/-}$ mice were digested into single cells, CD19^{-} non-B cells were identified into rDC, miDC and non-DCs. The percentages of SIGNR1^{+} rDC, SIGNR1^{+} miDC, SIGNR1^{+} macrophages and CD169^{+} macrophages were analyzed as indication. Data are representative results of three independent experiments. **b,** WT or *Signr1*$^{-/-}$ mice (n=3) were subcutaneously injected with 2 nmol ferritin-NP-eGFP. 4h after injection, inguinal LNs were digested into single cells, ferritin-NP-eGFP capture by DCs and CD169^{+} macrophages were presented and statistically analyzed. **c,** Inguinal LNs from WT or *Signr1*$^{-/-}$ mice were digested into single cells and incubated with ferritin-NP-eGFP or ferritin-NP-preS1-FITC *in vitro* (n=3). Ferritin-NP capture by

96 DCs and CD169^{+} macrophages were presented and statistically analyzed. In **b** and **c**,
97 data are representative results of two independent experiments, Data are shown as mean
98 ± SEM, statistical significance was determined by unpaired two-tailed *t*-test.
99

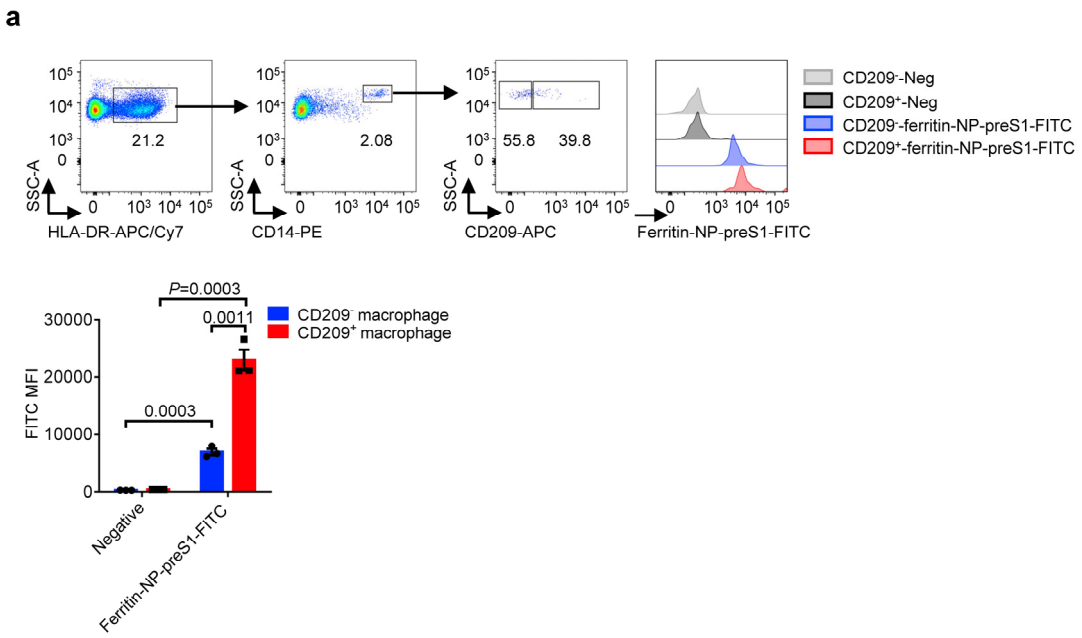

Supplementary Fig. 7: Ferritin-NP targets CD209$^+$ macrophages of human LNs. **a**, Human LNs were digested into single cells and incubated with ferritin-NP-preS1-FITC *in vitro* (n=3). HLA-DR$^+$ CD14$^+$ macrophages were gated and identified into CD209$^+$ and CD209$^-$ populations. The capture of ferritin-NP-FITC by CD209$^+$ or CD209$^-$ macrophage was detected and analyzed. Data are representative results of three independent experiments. Data are shown as mean ± SEM, statistical significance was determined by unpaired two-tailed *t*-test.

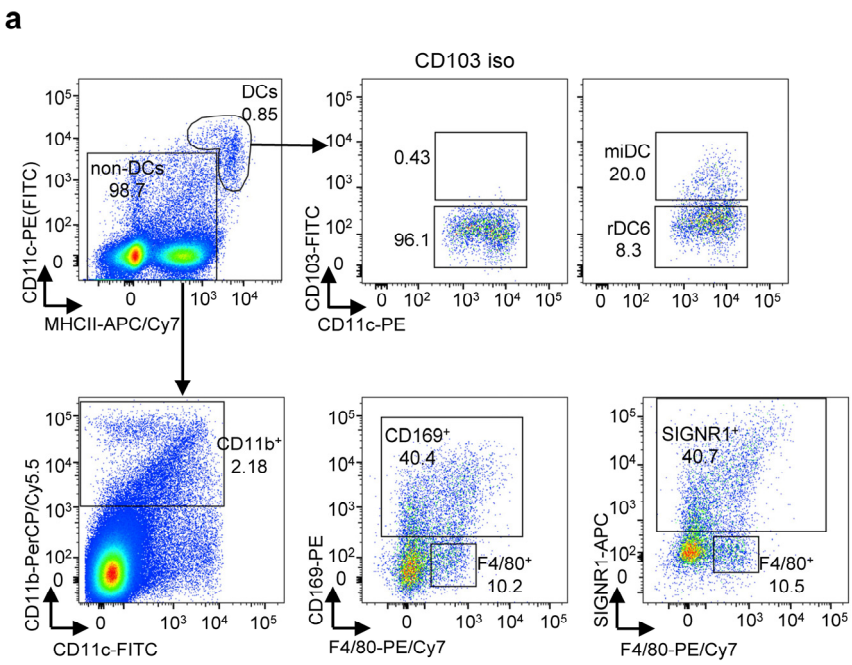

Supplementary Fig. 8: Gating strategy of antigen presenting cells in LNs after immunization.

a, The gating strategy of antigen presenting cells in dLNs of ferritin-NP vaccine immunized mice. $CD11c^{+/hi}MHCII^{+/hi}$ DCs were gated firstly and further analyzed by anti-CD103. $CD103^{+}$ migratory DCs and $CD103^{-}$ resident DCs were gated according to CD103 isotype. $CD11b^{+}$ non-DC cells were further classified into $F4/80^{+}$ macrophages and $CD169^{+}$ or $SIGNR1^{+}$ macrophages. Data are representative results of at least three independent experiments.

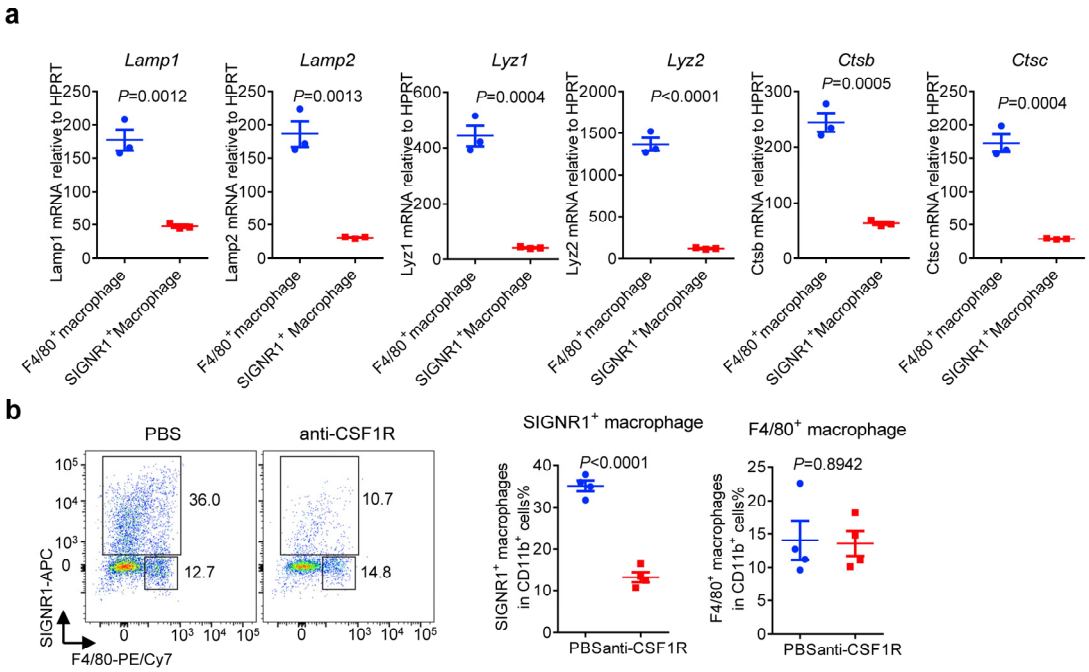

Supplementary Fig. 9: The characterization and depletion of SIGNR1+ macrophages in dLNs.

a, F4/80$^+$ macrophages and SIGNR1$^+$ macrophages were sorted from LNs of naïve mice, the gene expression of lysosome-associated membrane proteins (*Lamp1/Lamp2*), lysozyme (*Lyz1/Lyz2*) and lysosomal proteases (*Ctsb/Ctsc*) were detected by real-time PCR analysis (n=3). The data are representative results of two independent experiments. **b**, Depletion of SIGNR1$^+$ macrophages but not F4/80$^+$ macrophages upon anti-CSF1R treatment was determined by flow cytometry (n=4). Data are representative results of three independent experiments. Data are shown as mean ± SEM, statistical significance was determined by unpaired two-tailed *t*-test.

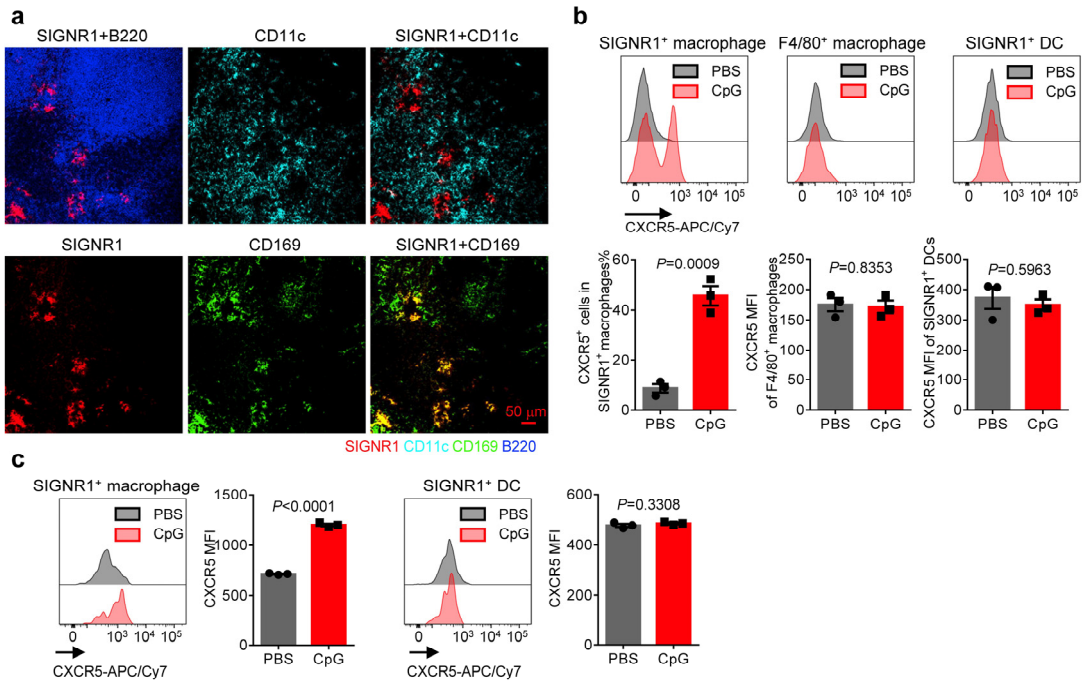

Supplementary Fig. 10: SIGNR1$^+$ macrophages upregulate CXCR5 after CpG immunization for follicular migration.

a, Naïve WT mice were subcutaneously immunized with 30 μg CpG-1826. Distribution of SIGNR1$^+$ (red), CD11c$^+$ (Cyan), CD169$^+$ (green) cells and B220$^+$ (blue) cells in iLNs were determined by immunofluorescence microscopy 3 days later. Data are representative results of three independent experiments. **b**, Naïve WT mice (n=3) were subcutaneously immunized with CpG-1826 adjuvant or PBS. The expression of CXCR5 by SIGNR1$^+$ macrophage, SIGNR1$^-$F4/80$^+$ macrophage, SIGNR1$^+$ DC in iLN were analyzed by flow cytometry 3 days later. Data are representative results of four independent experiments. **c**, SIGNR1$^+$ macrophages and SIGNR1$^+$ DCs were sorted from naïve WT mice LNs, cells were stimulated with 30 μg/ml CpG-1826 for 24 h *in vitro* (n=3), the expression of CXCR5 were analyzed. Data are representative results of three independent experiments. In **b** and **c**, data are shown as mean ± SEM, statistical significance was determined by unpaired two-tailed *t*-test.